Investigation of Brillouin Dynamic Grating in 4-LP-mode Fiber with a Ring-cavity Configuration for Distributed Temperature and Strain Sensing Application

Yinping Liu,[1,2] Guangyao Yang,[1,2] Ning Wang,[2] Lin Ma,[1,*] J. C. Alvarado-Zacarias,[2] J. E. Antonio-Lopez,[2] Pierre Sillard,[3] A. Amezcua-Correa,[3] R. Amezcua-Correa,[2] Xinyu Fan, [1] Zuyuan He,[1] and Guifang Li[2]

[1]State Key Laboratory of Advanced Optical Communication Systems and Networks, Shanghai Jiao Tong University, Shanghai 200240, China

[2] CREOL, The College of Optics and Photonics, University of Central Florida, Orlando, Florida, 32816, USA

[3] Prysmian Group, Parc des Industried Artois Flandres, Douvrin, 62138, France

ma.lin@sjtu.edu.cn

Abstract: We investigate temperature and strain dependency of Brillouin dynamic grating in 4-LP-mode fiber with a ring-cavity configuration. Sensitivities of 3.20 MHz/℃ and -0.0384 MHz/με are achieved. We demonstrate measurement with 300-m range and 1-m resolution.

OCIS codes: (290.5900) Scattering, stimulated Brillouin; (190.2055) Dynamic gratings; (060.2370) Fiber optics sensors

1. Introduction

Brillouin dynamic grating (BDG) generated by stimulated Brillouin scattering (SBS) effect is fully optical controllable and shows great potential in various applications, such as all-optical signal processing and microwave photonics [1]. It provides a novel approach to measure the fiber parameters, thus drowning much attention for the purpose of distributed fiber-optic sensors. With two counter-propagating pumps of one polarization and a probe of orthogonal polarization, the BDG can be generated and analyzed in a polarization-maintaining fiber (PMF) for dramatically improving the spatial resolution of Brillouin optical time domain analysis to 1 cm [2]. Due to the desirable dependences of the BDG frequency and Brillouin frequency shift (BFS) on temperature and strain, a complete temperature and strain discrimination was realized by simultaneously measuring the BDG frequency and BFS in a PMF [3]. However, the PMF-BDG scheme that requires an all-polarization-maintaining configuration will lead to a high overall cost. Alternatively, the BDG operation can also be conducted over a standard single-mode fiber (SMF) by controlling the polarization of pump and probe [4]. However, it is impracticable for distributed sensing due to the intrinsic random birefringence of SMF. Few-mode fiber (FMF), which is capable of supporting multiple spatial modes, has been regarded as a potential sensing media for distributed fiber-optic sensors. The BDG operation can be conducted in FMF by generating BDG through one mode and analyzing another mode [5]. Moreover, a multi-parameter sensor based on BDG operation in a polarization-maintaining elliptical-core two-mode fiber (e-core TMF) has been proposed [6]. By pumping through two orthogonal polarizations of the LP_{01} mode respectively and probing one polarization of the LP_{11} mode, the simultaneous temperature and strain sensing is realized with an accuracy of 1.6°C and 105 με, depends on the unique birefringence characteristics of e-core TMF. However, the BDG response to temperature and strain in a standard FMF, which is more practical and cost-effective, remains to be explored.

In this paper, we demonstrate BDG operation in a standard 4-LP mode fiber. A simplified ring-cavity configuration with single-ended pump is employed to efficiently built up a BDG over a 300-m distance. The generated BDG is then analyzed through three higher order modes with a 1-m spatial resolution, and the corresponding BDG frequency coefficients of temperature and strain are firstly investigated to the best of our knowledge. The temperature and strain sensitivities of 3.20 MHz/℃ and -0.0384 MHz/με are achieved by using LP_{01}-LP_{02} modes as the pump-probe pair. We also demonstrate the simultaneous strain and temperature sensing.

2. Principle

Figure 1(a) shows the operation principle of the proposed scheme. The BDG is generated by the SBS in mode *i* in the ring cavity and analyzed by the higher order mode *j*. When the pump at the frequency of v_i goes through the FMF in the anti-clockwise direction, the Stokes wave that experiences a frequency downshift of v_B will travel in the clockwise direction and stimulated emits the acoustic field in fiber. Thanks to the SBS process, the Stokes wave could accumulate enough gain from pump and lase stably when the pump power reaches the threshold value [7]. As a result, the BDG can be built up through the acoustic field. If a probe propagating in the same direction as the pump is launched into the ring-cavity in mode *j*, it can be reflected by the BDG when the pump-probe frequency deviation satisfying the phase-match condition:

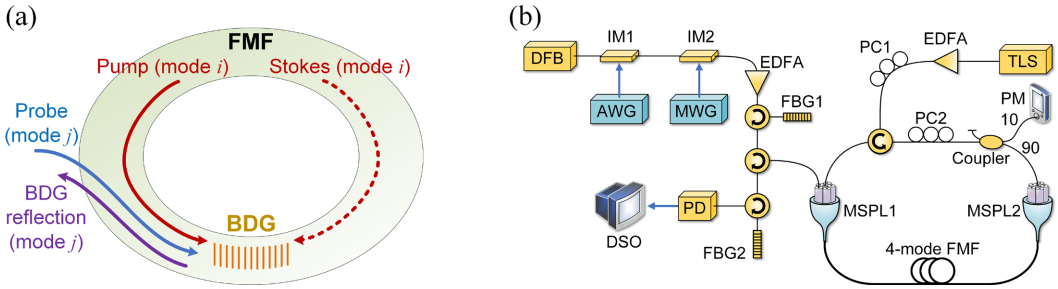

Fig. 1. (a) Operation principle of BDG operation in an FMF ring-cavity. (b) Experimental setup. DFB: distributed feed-back laser; IM: intensity modulator; EDFA: erbium-doped fiber amplifier; AWG: arbitrary waveform generator; MWG: microwave generator; FBG: fiber Bragg grating; TLS: tunable laser source; PM: power meter; MSPL: mode-selective photonic lantern; PD: photo-detector; PC: polarization controller; DSO: digital sampling oscilloscope.

$$\nu_D = \Delta n_{ij} \cdot \nu_i / n_i , \tag{1}$$

where ν_D is the frequency deviation between the pump and probe, called BDG frequency and Δn_{ij} is regarded as the intermodal birefringence. When the BDG is analyzed by mode j, the relationship between the variation of BDG frequency ($\Delta\nu_D$) and the change of temperature and axial strain (ΔT, $\Delta\varepsilon$) can be expressed as:

$$\Delta\nu_D = C_T^{i,j} \cdot \Delta T + C_\varepsilon^{i,j} \cdot \Delta\varepsilon, \tag{2}$$

where C_T and C_ε are the temperature and strain coefficients. As a result, the temperature and strain profile along the fiber can be obtained through the variation of BDG frequency. Furthermore, the simultaneously temperature and strain sensing could be expected in the case that the temperature and strain coefficients of different pump-probe pairs show a significant distinct [8].

3. Experimental setup and results

The experimental setup is shown in Fig. 1(b). A tunable laser source (TLS) was used as the light source for pump and the output light was amplified by an erbium-doped fiber amplifier (EDFA). The polarization states between the pump and Stokes wave are aligned using polarization controllers (PCs) in order to maximize the SBS gain. The fiber under test (FUT) is a 400-meter-long step-index (SI) 4-LP-mode FMF with a core diameter of 15 μm which can support six degenerate modes (LP_{01}, LP_{11a}, LP_{11b}, LP_{21a}, LP_{21b} and LP_{02}). A pair of mode-selective photonic lanterns (MSPL) were used to evolve the input fundamental mode into the desired mode of the FMF [9]. The pump was launched into the LP_{01} port of MSPL1 through a circulator and the backscattering Stokes wave was amplified due to the intramodal SBS effect in the ring cavity. In our experiment, the pump power was set to be 630 mW and the power of Stokes wave was measured to be 230 mW. A distributed feed-back (DFB) laser was used as the laser source for BDG analyzing. The output of DFB laser was modulated into pulses by an intensity modulator (IM) with a repetition rate of 250 kHz and a width of 10 ns, corresponding to a 1-m spatial resolution. The other IM in cooperation of a fiber Bragg grating (FBG) was employed to perform a single sideband (SSB) modulation on the interrogation pulses. By sweeping the SSB modulation frequency, the BDG reflection spectra along the fiber can be

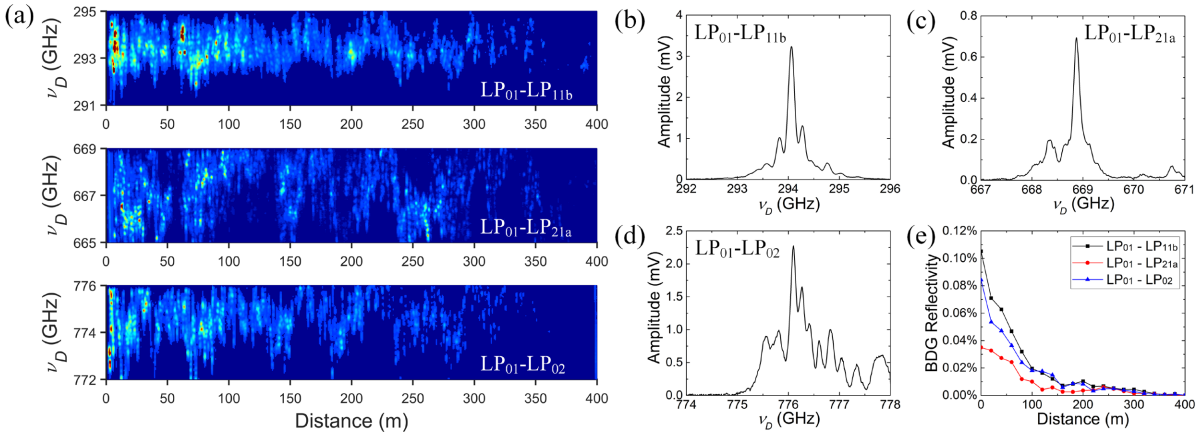

Fig. 2. (a) BDG spectrum distributions along the FUT for each pump-probe combination, local BDG reflection spectra at the distance of 200 m for pump-probe pairs of (b) LP_{01}-LP_{11b}, (c) LP_{01}-LP_{21a}, and (d) LP_{01}-LP_{02} mode, and (e) BDG reflectance versus fiber length for different pump-probe pairs.

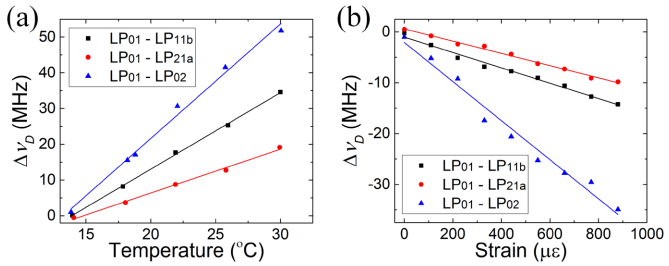

Fig. 3. Measured $\Delta\nu_D$ as a function of (a) temperature and (b) strain.

Table 1. The temperature and strain coefficients

Probe	C_T (MHz/°C)	C_ε (MHz/με)	Error (MHz)
LP_{11b}	2.14	-0.0143	0.52
LP_{21a}	1.22	-0.0121	1.92
LP_{02}	3.20	-0.0384	0.68

obtained. The pulses were amplified to a peak power of 3.5 W by the EDFA and then converted into a specific high-order mode by MSPL1 to analyze the BDG. Here, LP_{11b}, LP_{21a} and LP_{02} modes are experimentally selected to be probes as they have relatively low insertion losses. The reflection of BDG was detected by a photodetector after passing the other FBG filter, and the output of photodetector was sampled by a digital sampling oscilloscope (DSO) with a 1000-times average to improve SNR.

Figure 2(a) shows the BDG reflection spectra distributions along the FUT for different pump-probe combinations. It can be observed that the phase-match condition can be approximately satisfied when the frequency deviation between pump in LP_{01} mode and probes in LP_{11b}, LP_{21a} and LP_{02} mode were tuned to be around 293.5, 667 and 774 GHz respectively, corresponding to an intermodal birefringence of 2.19e-3, 4.98e-3, and 5.77e-3, respectively. Due to the nonuniformity along the FUT introduced by the fabrication and winding process, the dominant reflection peak at different positions changes randomly within a range of 4 GHz, corresponding to an effective refractive index variation of 3e-5. Figures 2 (b)-(d) show the local BDG reflection spectra for different pump-probe pairs at the distance of 200 m, where multiple reflection peaks are observed within a 3-GHz range, which also attributes to the fiber nonuniformity. The relationship between BDG reflectivity and distance for different pump-probe pairs are calculated and shown in Fig. 2(e). It can be observed that BDGs were built up at first 300-m distance of FUT and attenuated rapidly along the distance due to the depletion of pump power. Besides, the reflectivity of different pump-probe pairs shows significant discrepancy, which is mainly determined by the overlap integral of optical and acoustic fields for different modes.

The temperature and strain of a 2-m FUT at a distance of 200 m were controlled in order to investigate the temperature and strain coefficients. Figure 3 shows the calculated frequency shift $\Delta\nu_D$ as a function of (a) temperature and (b) strain with different pump-probe pairs, while the obtained temperature and strain coefficients as well as measurement error of $\Delta\nu_D$ are shown in Tab. 1. By using the probe of LP_{02} mode, a temperature and strain sensitivities of 3.20 MHz/°C and -0.0384 MHz/με are achieved respectively. The variation of errors for different pump-probe pairs mainly attributes to the difference of reflectivity. Moreover, by using both LP_{11b} and LP_{02} modes as probes, simultaneously temperature and strain sensing is demonstrated with a deteriorated accuracy of 0.61 °C and 60.7 με, thanks to the distinctive coefficients.

4. Conclusion

We have experimentally demonstrated a BDG operation in a conventional 4-LP mode FMF for distributed temperature and strain sensing application. With a simplified fiber ring-cavity configuration, the BDG is efficiently built up over a distance of 300 m by employing a single-end pump through LP_{01} mode and analyzed through three higher modes respectively with a spatial resolution of 1 m. The temperature and strain coefficients of the BDG frequency shift with different high-order modes as probes are investigated in a conventional FMF for the first time. By using the modes combination of LP_{01}-LP_{02}, the sensitivities of 3.20 MHz/°C and -0.0384 MHz/με are achieved.

Acknowledgement

This work is supported by the National Key R&D Program of China under grant 2018YFB1801000 and National Natural Science Foundation of China under Grant 61775138, 61775132, 61975116. Y. Liu acknowledges the support of the China Scholarship Council (CSC).

References

[1] M. Santagiustina et al., Sci. Rep. **3**, p. 1594, 2013.
[2] K. Y. Song et al., J. Lightwave Technol. **28**(14), p.2062, 2010.
[3] W. Zou et al., Opt. Express **17**(3), p. 1248, 2009.
[4] K. Y. Song, Opt. Lett. **36**(23), p. 4686, 2011.
[5] A. Li et al., Opt. Lett. **40**(7), p. 1139, 2015.
[6] Y. H. Kim et al., Opt. Lett. **42**(15), p. 3036, 2017.
[7] N. Wang et al., Proc. CLEO'2019, paper SM1L.1.
[8] W. Jin et al., Opt. Eng. **36**(2), p. 598, 1997.
[9] A. M. Velazquez-Benitez et al., Opt. Lett. **40**(8), p. 1663, 2015.